Geochemistry Geophysics Geosystems G3
AN ELECTRONIC JOURNAL OF THE EARTH SCIENCES
Published by AGU and the Geochemical Society

Article
Volume 4, Number 4
8 April 2003
1033, doi:10.1029/2002GC000440
ISSN: 1525-2027

Paleomagnetic record at ODP Site 980 (Feni Drift, Rockall) for the past 1.2 Myrs

J. E. T. Channell
Department of Geological Sciences, P.O. Box 112120, 241 Williamson Hall, University of Florida, Gainesville, Florida 32611, USA (jetc@ufl.edu)

M. E. Raymo
Department of Earth Sciences, Boston University, 685 Commonwealth Avenue, Boston, Massachusetts 02215, USA (raymo@bu.edu)

[1] A detailed record of variations in the direction and intensity of the geomagnetic field over the past 1.2 Myrs has been obtained from an ~120-m-thick sedimentary section cored at ODP Site 980 on the Feni Drift (North Atlantic). The record has high resolution due to high mean sedimentation rates (11.3 cm/kyr for the Brunhes Chron and 5.5 cm/kyr for the Matuyama Chron), paleomagnetic measurements every 1 cm along u-channel samples, and high quality isotopic age control. The Iceland Basin Event is manifest by virtual geomagnetic poles crossing the equator at ~190 ka. The base of the recovered section lies immediately below the Cobb Mountain Subchronozone that occurs within marine isotope stage 35. Normalized remanence data can be correlated to paleointensity records from ODP Sites 983 and 984 (~700 km to the NW from Site 980) and with lower resolution paleointensity data from the Pacific Ocean. Differences between the Site 980 paleointensity record and the Pacific records are attributed to variable sedimentation rates, variable quality age control, and inadequacies in the normalization procedure used to derive the paleointensity proxies.

Components: 5511 words, 10 figures, 1 table, 2 datasets.

Keywords: Paleomagnetism; paleointensity; Brunhes and Matuyama Chrons; oxygen isotopes; Rockall Plateau; North Atlantic.

Index Terms: 1520 Geomagnetism and Paleomagnetism: Magnetostratigraphy; 1521 Geomagnetism and Paleomagnetism: Paleointensity; 1535 Geomagnetism and Paleomagnetism: Reversals (process, timescale, magnetostratigraphy).

Received 10 September 2002; **Revised** 30 December 2002; **Accepted** 13 January 2003; **Published** 8 April 2003.

Channell, J. E. T., and M. E. Raymo, Paleomagnetic record at ODP Site 980 (Feni Drift, Rockall) for the past 1.2 Myrs, *Geochem. Geophys. Geosyst.*, *4*(4), 1033, doi:10.1029/2002GC000440, 2003.

1. Introduction

[2] Ocean Drilling Program (ODP) Site 980 was drilled in July 1995 off the eastern edge of the Rockall Plateau at 55.49°N, 14.70°W (Figure 1) in a water depth of 2170 m. The ~120 m section recovered at the site comprises Quaternary light gray to dark gray nannofossil oozes and clayey nannofossil oozes [*Shipboard Scientific Party*, 1996]. The base of the recovered section lies just below the Cobb Mountain Subchronozone (~1.2 Ma), giving an overall mean sedimentation rate of ~10 cm/kyr. The composite section at Site 980 is a splice of the three holes drilled at the site. It was

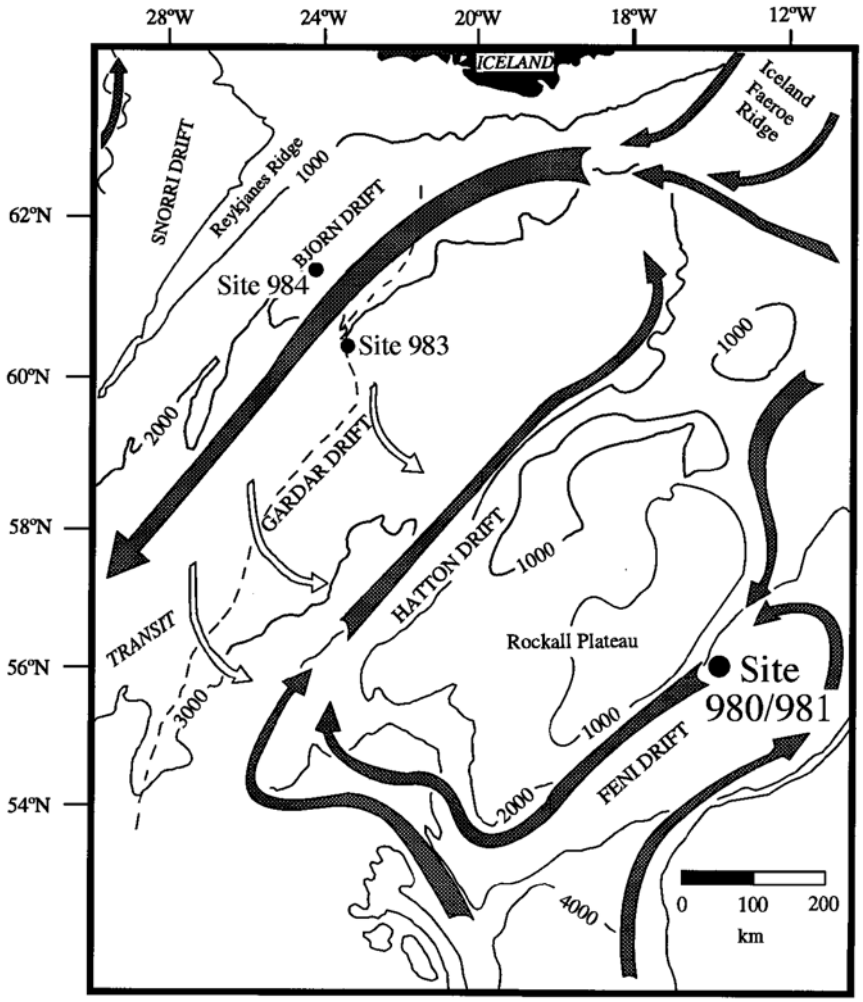

Figure 1. Location map for ODP Site 980/981. Bathymetry in meters. Dashed line indicates crest of Gardar Drift. Arrows indicate inferred bottom current flows [after *Manley and Caress*, 1994; *McCave et al.*, 1980].

based on shipboard hole-to-hole correlation of susceptibility, gamma-ray attenuation porosity (GRAPE), natural gamma radiation, and spectral reflectance data [*Shipboard Scientific Party*, 1996]. The composite section provides an optimal record of the sediment sequence [see *Hagelberg et al.*, 1992].

[3] ODP Site 981 was drilled approximately 3 km SE of Site 980. The rationale for the location of the two sites was based on seismic evidence for higher Brunhes sedimentation rates at Site 980, but higher Matuyama sedimentation rates at Site 981 [*Shipboard Scientific Party*, 1996]. Three holes were drilled at Site 981, and the composite section was compiled as a splice of the three holes, as for Site 980.

[4] The age model at Site 980/981 is based on the oxygen isotope data from the benthic foraminifera *Cibicidoides wuellerstorfi* [*Oppo et al.*, 1998; *McManus et al.*, 1999; *Flower et al.*, 2000]. Oxygen isotope data for Site 980 do not extend below 98.50 meters composite depth (mcd), equivalent to 950 ka. The age model below this depth at Site 980 is based on oxygen isotope data from Site 981, and the correlation between Sites 980 and 981 accomplished by correlation of shipboard records of susceptibility, gamma-ray attenuation porosity (GRAPE), natural gamma radiation, and spectral reflectance data [*Shipboard Scientific Party*, 1996].

[5] Here we report a magnetic study based on u-channel samples collected from the composite section at Site 980. We construct our age model

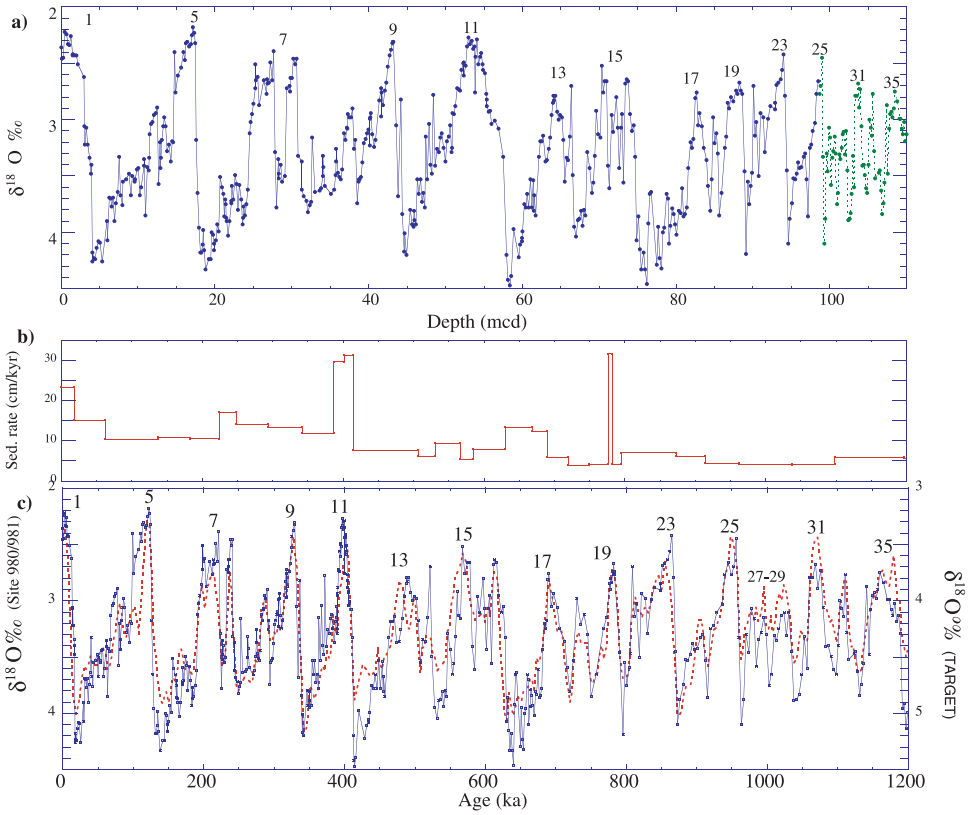

Figure 2. (a) Benthic $\delta^{18}O$ data versus depth for Site 980 [*Oppo et al.*, 1998; *McManus et al.*, 1999; *Flower et al.*, 2000] and Site 981 (dashed line). (b) Interval sedimentation rates according to the age model derived from the fit in Figure 2c. Spikes in sedimentation rate in MIS11 and MIS 19 are implied. (c) Benthic $\delta^{18}O$ data versus depth for ODP Site 980 (continuous line) correlated to the chronology of *Shackleton et al.* [1990] as defined by his TARGET curve (dashed line).

for Site 980 by matching the Site 980/981 benthic $\delta^{18}O$ record to the chronology of *Shackleton et al.* [1990] as defined by his TARGET curve (http://delphi.esc.cam.ac.uk/coredata/v677846.html) shown in Figure 2c. The target curve in the interval of interest comprises data from piston core V19-30 [*Shackleton and Pisias*, 1985] and from ODP Site 677 [*Shackleton et al.*, 1990]. The matching of the Site 980 $\delta^{18}O$ record to the TARGET curve yields sedimentation rates mainly in the 5–17 cm/kyr range, with rates exceeding 20 cm/kyr in the Holocene, in marine isotope stage (MIS) 11 and MIS 19 (Figure 2b).

2. Magnetic Data

[6] The magnetic polarity stratigraphies for Site 980, and other sites drilled south of Iceland during ODP Leg 162, were based on shipboard pass-through measurements of archive-halves of core sections, and discrete samples collected from the working-halves of core sections [*Channell and Lehman*, 1999]. The positions of the Matuyama-Brunhes boundary and the boundaries of the Jaramillo Subchronozone were determined from these data.

[7] In an effort to further define the paleomagnetic record at Site 980, we have used u-channels, plastic containers with a 2 × 2 cm square cross-section and the same length as the core sections (usually 150 cm), to continuously sample the composite section. U-channels were stepwise demagnetized using alternating fields (AF) in the 20–80 mT peak field range. The remanent magnetization was measured after each demagnetiza-

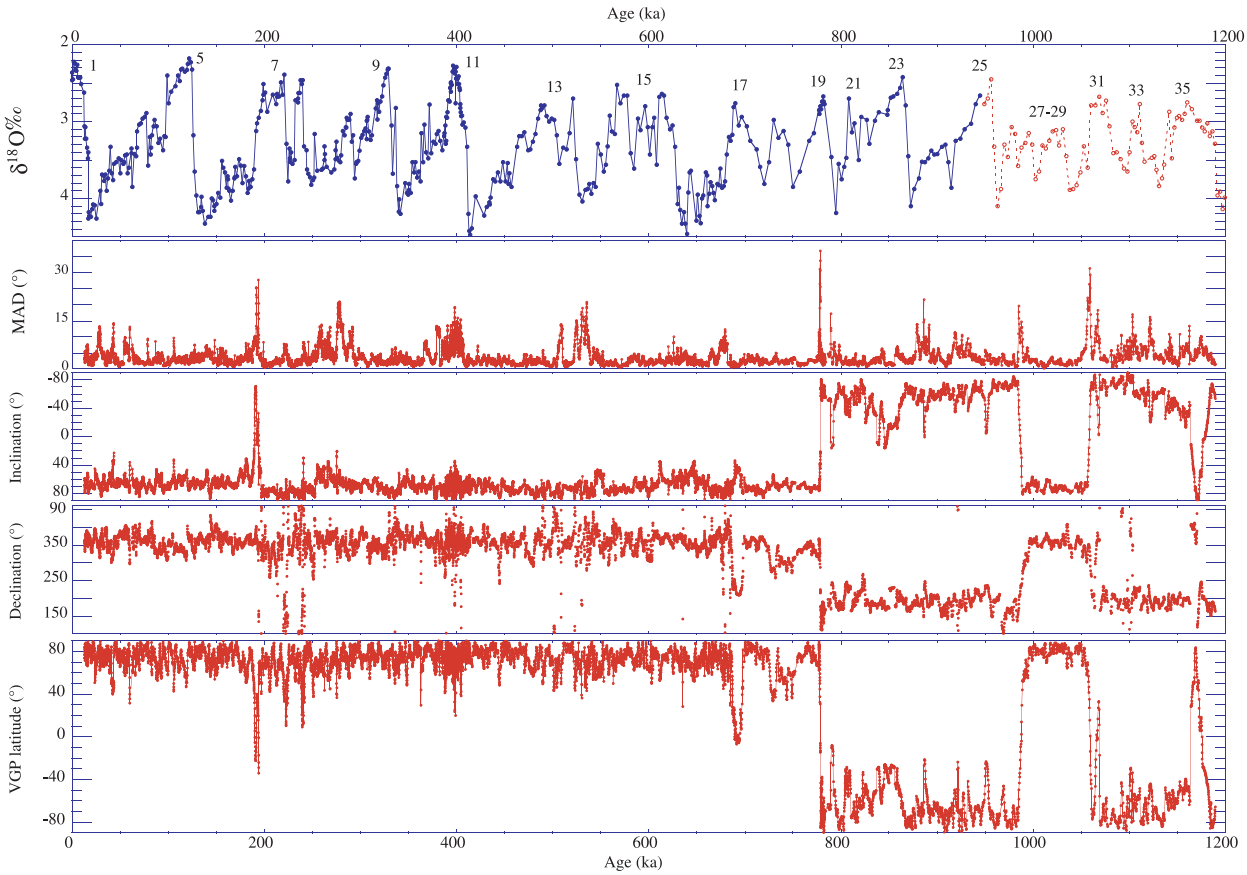

Figure 3. ODP Site 980/981 data placed on the age model from Figure 2. Benthic $\delta^{18}O$ data from Site 980 [*Oppo et al.*, 1998; *McManus et al.*, 1999; *Flower et al.*, 2000] and the continuation at Site 981 (dashed line). Component declinations and inclinations calculated for the 30–80 mT demagnetization interval, maximum angular deviation (MAD) values, and virtual geomagnetic polar (VGP) latitudes. See data set 1 of the auxiliary material (available in the HTML version of this article at http://g-cubed.org).

tion step at 1 cm intervals on a 2G Enterprises pass-through magnetometer designed for u-channel samples [*Weeks et al.*, 1993]. Component directions were calculated by applying the standard least squares method [*Kirschvink*, 1980] to the 30–80 mT demagnetization interval each 1 cm down-section. The response function of the u-channel magnetometer has a width at half-height of ~4 cm so that adjacent measurements are not independent and some smoothing is inherent in the measurement procedure.

[8] Component declination and inclination define the Matuyama-Brunhes boundary within MIS 19, and the boundaries of the Jaramillo Subchronozone within MIS 27 and MIS 31 (Figure 3). Within the Brunhes Chronozone, the Iceland Basin Event correlates to the MIS 6/7 boundary (~190 ka). In addition, virtual geomagnetic polar (VGP) latitudes cross the (magnetic) equator at ~690 ka within MIS 17. The Cobb Mountain Subchronozone occurs within MIS 35.

[9] Maximum angular deviation (MAD) values give a measure of the uncertainty in estimation of component directions [see *Kirschvink*, 1980]. For Site 980, MAD values are generally less than 10° (Figure 3). From observation of orthogonal projections of AF demagnetization data, the higher MAD values (>15°) close to "events" or polarity reversals are due to superposition of normal and reverse magnetization directions (Figure 4a). The apparent superposition of normal and reverse magnetization directions implies non-instantaneous remanence acquisition and a finite lock-in function. Rather than computing component directions in a constant

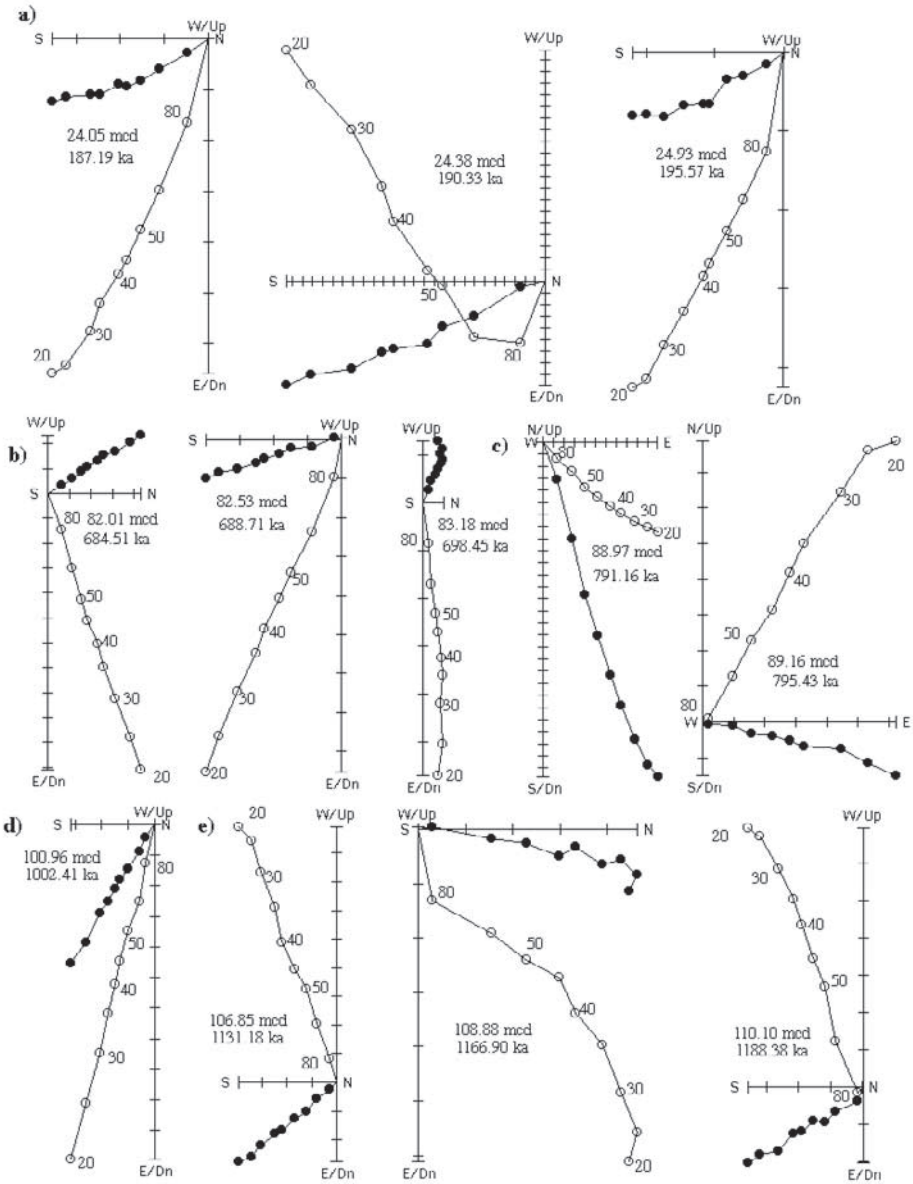

Figure 4. Site 980: orthogonal projection of alternating field demagnetization data for samples: (a) bounding and within the Iceland Basin Event at ~190 ka, (b) recording "event" at ~690 ka within marine isotope stage 17, (c) recording the positive inclination interval immediately below the Matuyama-Brunhes boundary, (d) recording the Jaramillo Subchronozone, (e) bounding and within the Cobb Mountain Subchronozone. Open and closed symbols indicate projection on the vertical and horizontal planes, respectively. The position of the sample in meters composite depth (mcd), and the estimated age are indicated. The peak alternating fields range from 20 mT to 80 mT. Scale divisions represent 1 mA/m for all projections other than 24.38 mcd (Figure 4a) where divisions represent 0.1 mA/m.

peak field interval (30–80 mT in this case), lower MAD values could have been obtained by picking components individually from the 10,300 individual orthogonal projections! Observations of orthogonal projections in critical intervals indicate that magnetization components are usually adequately defined. For example, for the Iceland Basin Event at ~190 ka, multicomponent magnetizations are present in the 24–25 meters composite depth (mcd) interval (Figure 4a), however, the presence

of the "reverse" components is unequivocal (e.g., sample at 24.38 mcd in Figure 4a). Within MIS 17, an apparent "event" is manifest mainly as a change in declination within the lower half of a single core section (980A-8H-3) in the 82.30–83.16 mcd interval (Figures 3 and 4b). Orthogonal projections, for a low inclination interval just below the Matuyama-Brunhes boundary (Figure 4c), for the Jaramillo Chron (Figure 4d) and for the Cobb Mountain Subchronozone (Figure 4e) indicate adequate definition of component directions during brief "events" and subchrons.

3. Paleointensity Determinations

[10] Paleointensity proxies in sediments have been constructed by normalizing NRM intensities using the intensities of laboratory-imposed remanences such as isothermal remanence (IRM) or anhysteretic remanence (ARM). The procedure works well if the normalizer (ARM or IRM) magnetizes the same grains that carry NRM, and if the remanence carrier is magnetite in the single-domain or pseudo-single-domain (rather than multidomain) grain-size range. In these favorable circumstances, the normalization procedure compensates for down-core changes in concentration of remanence-carrying grains. *King et al.* [1983] placed the use of ARM as the normalizer on a firm theoretical and empirical basis. Changes in concentration of remanence-carrying grains should not exceed an order of magnitude, as measured by susceptibility and ARM and IRM intensities, due to the effect of particle interactions on ARM acquisition [*King et al.*, 1983; *Tauxe*, 1993].

[11] At Site 980, the lack of evidence for high-coercivity magnetic minerals in orthogonal projections of AF demagnetization data, indicate magnetite as the principal remanence carrier (Figures 4). Hysteresis ratios (Figure 5a) are clustered in the pseudo-single-domain grain size field of *Day et al.* [1977]. Following *King et al.* [1983], plots of anhysteretic susceptibility (k_{arm}) against susceptibility (k) provide estimates of magnetite grain size that are largely less than 20 μm, other than within MIS 12 (Figure 5b). Values of susceptibility, IRM and ARM reach a maximum within MIS 12 and a minimum within MIS 11 (Figure 6). MIS 11 and

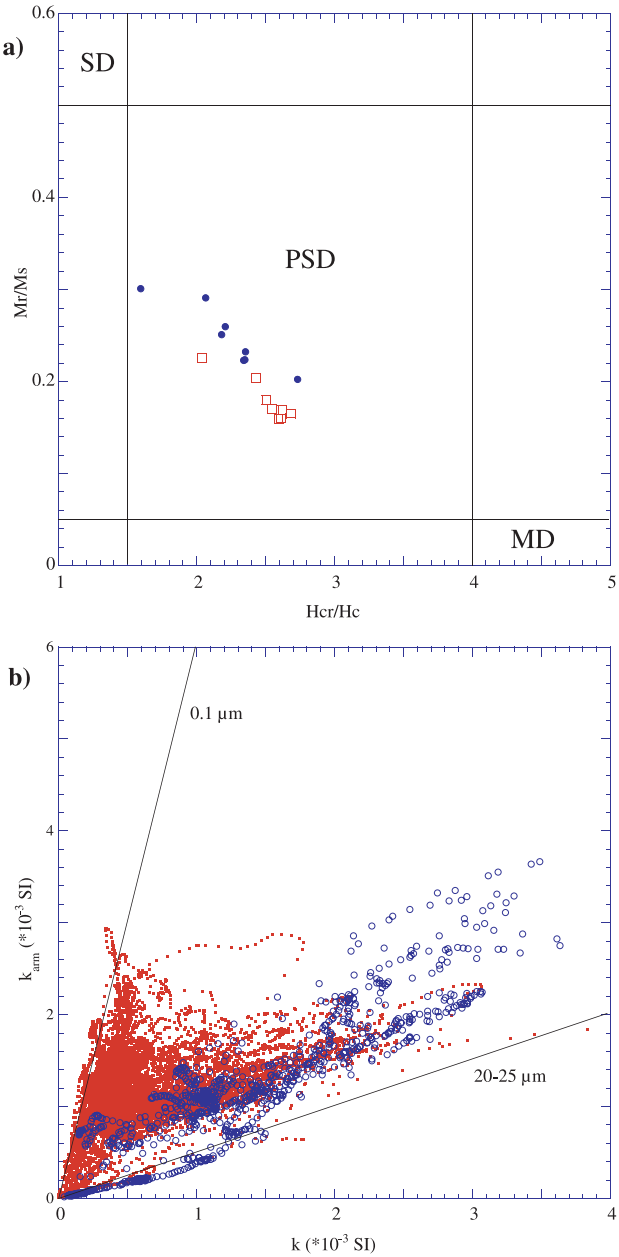

Figure 5. (a) Hysteresis ratios lie in the pseudo-single-domain (PSD) field of *Day et al.* [1977] when measured at 300 K (open squares) and 90 K (closed circles). (b) Plot of anhysteretic susceptibility (k_{arm}) against volume susceptibility (k). Data from marine isotope stage (MIS) 12 and the MIS 11/12 termination are shown as large open symbols. Magnetite grain-size estimates from *King et al.* [1983].

MIS 12 were extreme interglacial/glacial stages [*Howard*, 1997], and at Site 980 the MIS11/12 boundary coincides with an abrupt change in percent IRD and sea-surface temperature proxies

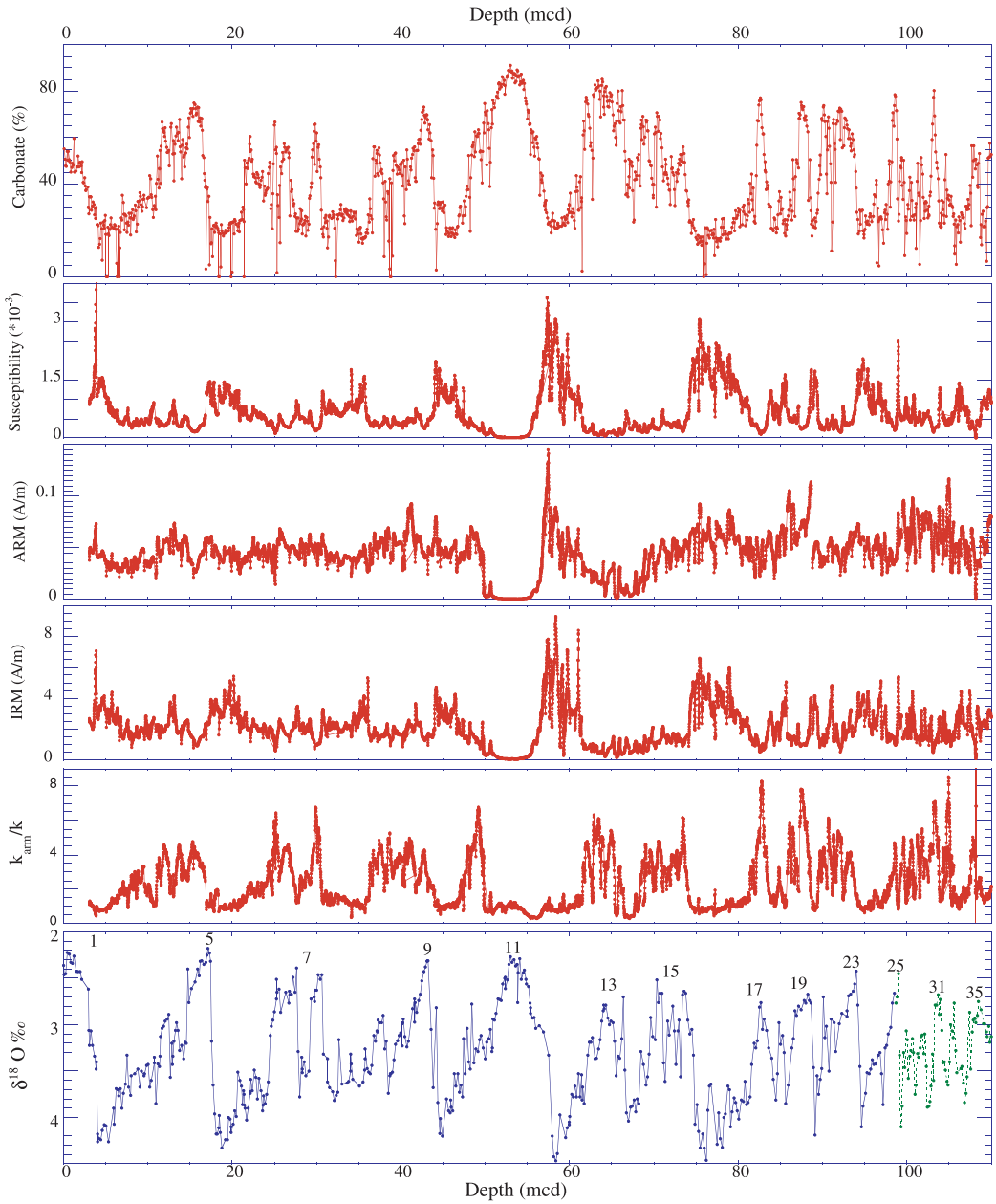

Figure 6. Site 980/981: Percentage carbonate data [from *Ortiz et al.*, 1999], volume magnetic susceptibility (k), anhysteretic remanence (ARM), isothermal remanence (IRM), anhysteretic susceptibility divided by susceptibility (k_{arm}/k), and benthic $\delta^{18}O$. ARM and IRM after demagnetization at peak fields of 35 mT. Benthic $\delta^{18}O$ data for Site 980 [*Oppo et al.*, 1998; *McManus et al.*, 1999; *Flower et al.*, 2000] and Site 981 (dashed line).

[*Oppo et al.*, 1998]. Within MIS 11, sedimentation rates reach 30 cm/kyr (Figure 2b) and carbonate percentages reach ~90% (Figure 6). The very low concentration of magnetic minerals in MIS 11 can be attributed to enhanced surface water productivity (carbonate production) and diminished ice rafting. Conversely, the high magnetic concentration in MIS 12 can be attributed to enhanced ice rafting and diminished sea-surface temperatures [*Oppo et al.*, 1998].

[12] The ratio of anhysteretic susceptibility to susceptibility (k_{arm}/k), a commonly used grain size proxy for magnetite, shows high values (smaller magnetite grain sizes) during interglacial stages (Figure 6). The exception is MIS 11 where all

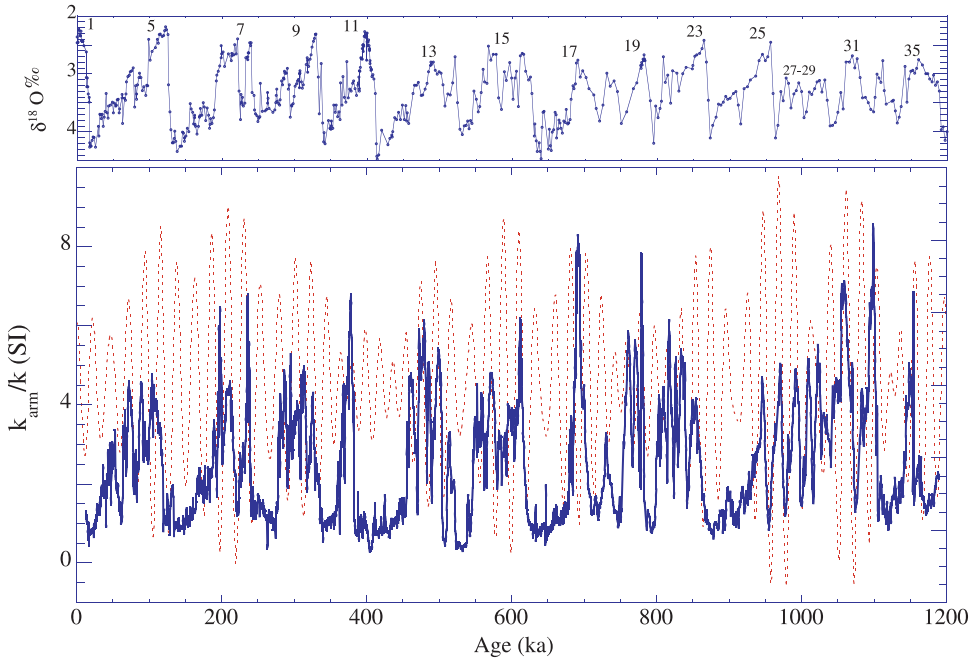

Figure 7. (top) Benthic $\delta^{18}O$ data for Site 980/981 (partially from *Oppo et al.* [1998], *McManus et al.* [1999], and *Flower et al.* [2000]). (bottom) Ratio of volume anhysteretic susceptibility (k_{arm}) to volume susceptibility (k) for the Site 980 plotted against age (continuous line). Orbital solution for precession from *Laskar et al.* [1993] (dashed line).

magnetic concentration parameters have values close to zero. When placed on the age model, values of k_{arm}/k in interglacial stages (other than MIS11) are relatively high and show precessional-scale variability (Figure 7). This variability could be attributed to grain size changes produced by bottom-current fluctuations during interglacial stages. Low values of k_{arm}/k usually correspond to glacial stages, and do not show obvious precessional-scale variability. The millennial-scale variability in percent IRD recognized at Site 980 [*McManus et al.*, 1999; *Oppo et al.*, 1998] is not clearly manifest in the magnetic parameters (Figure 6), although there is higher frequency variability in k_{arm}/k during glacial stages compared to interglacial stages (Figure 7).

[13] In the MIS 11–13 (350–460 ka) interval, magnetic concentration parameters vary by more than an order of magnitude (Figure 6) and magnetite grain size estimates exceed 20 μm (Figure 5b). For this reason, paleointensity proxies in this interval are likely to be unreliable due to the effect of particle interaction and grain size on remanence acquisition. We construct our paleointensity proxies for Site 980 by averaging the nine values of NRM/ARM and NRM/IRM calculated for each demagnetization step in the 25–60 mT peak field range. Both NRM/ARM and NRM/IRM are essentially invariant with increasing demagnetization field, indicating that the coercivity spectrum in the 25–60 mT peak field range is similar for ARM, IRM and NRM. Mean NRM/ARM and mean NRM/IRM give consistent proxies for part of the record (Figure 8b), however, discrepancies between the two proxies are apparent in peak interglacial stages (MIS 1, 11, 19) and peak glacials (MIS 2, 6, 12, 18) (boxed in Figure 8b). The mean NRM/IRM record shows power at orbital periods, derived from IRM, that is largely absent in mean NRM/ARM (Figure 9a). This leads to significant coherence between NRM/IRM and IRM at orbital periods (Figure 9b). Coherence between NRM/ARM and ARM is below the 95% confidence level for most of the record. Where coherence between NRM/ARM and ARM exceeds the 95% confidence level, power in NRM/ARM is low (Figure 9a). For this reason, we consider NRM/ARM less contaminated by climate than NRM/IRM, and adopt mean NRM/ARM as the paleointensity proxy at Site 980.

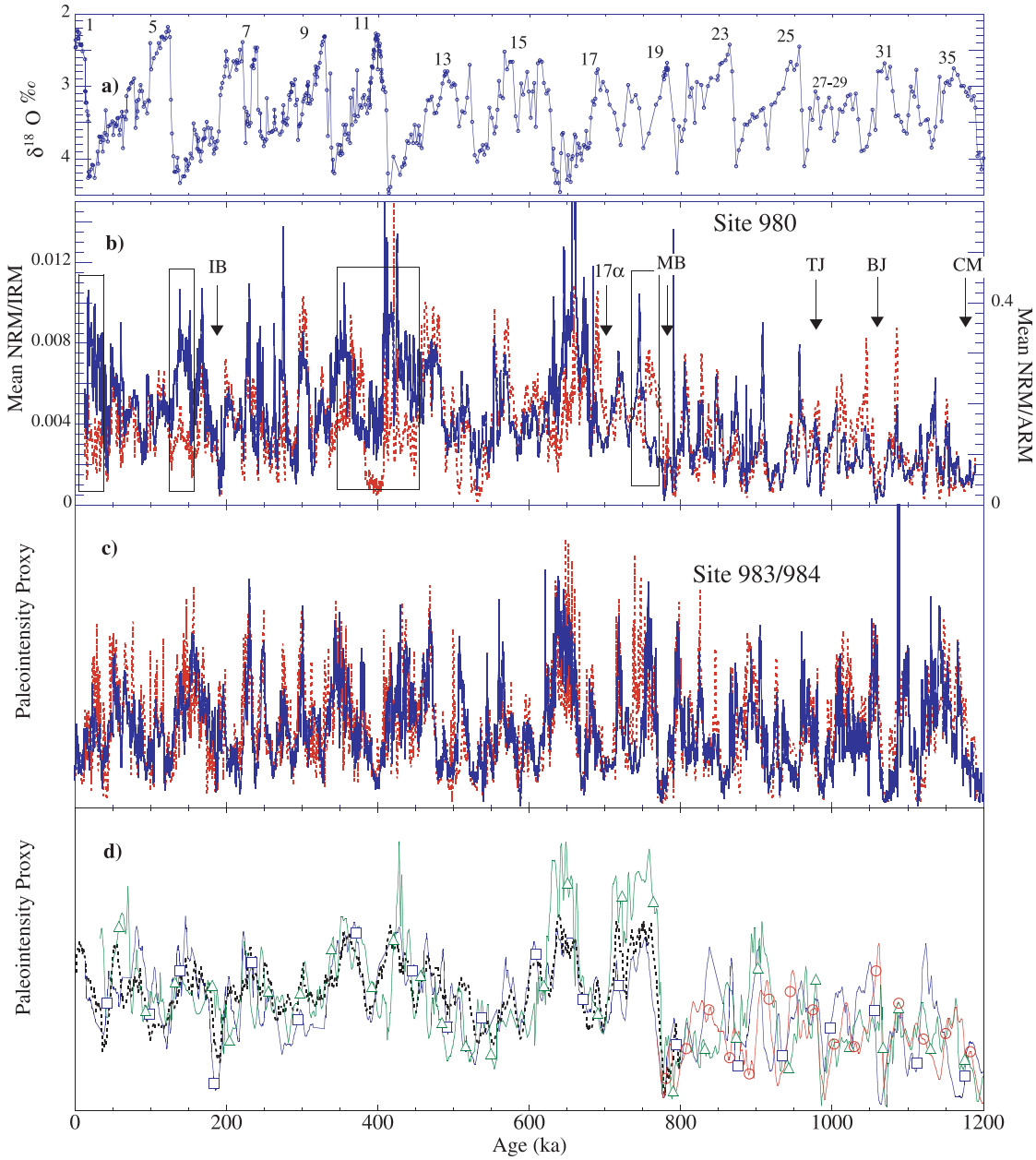

Figure 8. (a) Benthic $\delta^{18}O$ data for Site 980/981 (partially from *Oppo et al.* [1998], *McManus et al.* [1999], and *Flower et al.* [2000]) placed on the new age model. (b) Paleointensity proxies for Site 980: mean NRM/ARM (continuous line) and mean NRM/IRM (dashed line). Large discrepancies (boxed) are apparent in peak interglacial stages (MIS 1, 11, 19) and peak glacials (MIS 2, 6, 12, 18). Reversals and excursions: IB, Iceland Basin Event; 17α, MIS 17 "event"; MB, Matuyama-Brunhes boundary; TJ, top Jaramillo; BJ, base Jaramillo; CM, Cobb Mountain. See data set 2 of the auxiliary material. (c) Paleointensity proxies (arbitrary units) for Site 984 (dashed line) and Site 983 (continuous line) [*Channell*, 1999; *Channell et al.*, 1998; *Channell and Kleiven*, 2000]. (d) Other paleointensity estimates: Circles: Ontong-Java stack [*Kok and Tauxe*, 1999]; Squares: California Margin ODP Site 1021 [*Guyodo et al.*, 1999]; Triangles: Equatorial Pacific ODP Leg 138 [*Valet and Meynadier*, 1993]; Dashed line: Sint-800 composite stack [*Guyodo and Valet*, 1999].

[14] The paleointensity record from Site 980 is compared with those from Sites 983/984 (Figure 8c), and with the Sint-800 global stack [*Guyodo and Valet*, 1999] and records from the Pacific Ocean [*Valet and Meynadier*, 1993; *Meynadier et al.*, 1995; *Guyodo et al.*, 1999; *Kok and Tauxe*, 1999] (Figure 8d). The paleointensity record from Site 980, particularly the NRM/ARM record, is a rea-

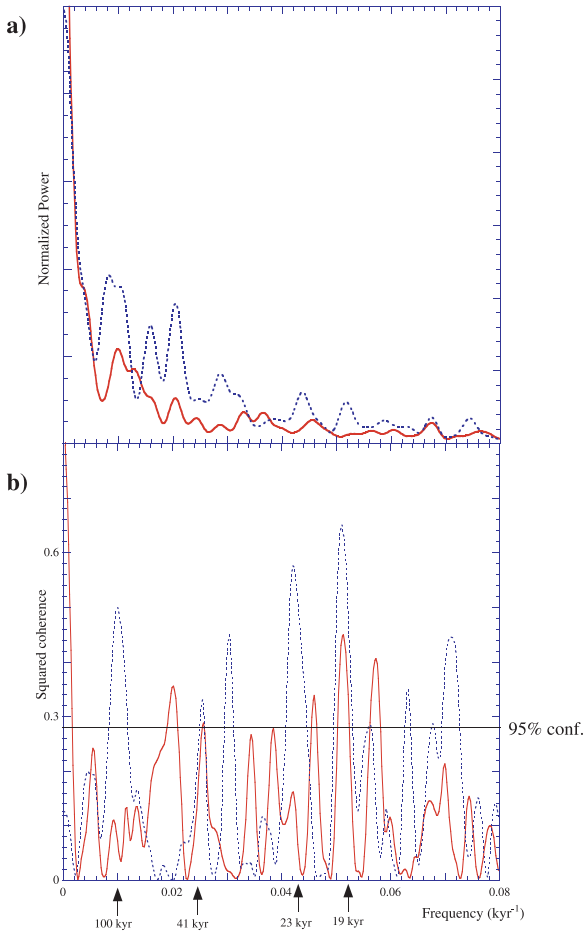

Figure 9. Site 980: (a) power spectra for mean NRM/ARM (continuous line) and mean NRM/IRM (dashed line) and (b) squared coherence for NRM/ARM and ARM_{35mT} (continuous line) and NRM/IRM and IRM_{35mT} (dashed line). Analysis using AnalySeries software [*Paillard et al.*, 1996] and the Blackman-Tukey method with a Bartlett window.

sonable match to the records from Sites 983/984. The larger-scale features in the Site 980/983/984 records are seen in the records from the Pacific Ocean (Figure 8d). The lower mean paleointensity values for the Matuyama Chron, relative to the Brunhes Chron, for Site 980 (Figure 8b) and for the Pacific records (Figure 8d) may be due to uncleaned Brunhes-age viscous remanence (VRM) that is not apparent in orthogonal projections of demagnetization data (Figure 4).

4. Discussion

[15] The correlation of Plio-Pleistocene isotopic stages to polarity chrons and subchrons has been established using data from Deep Sea Drilling Project (DSDP) Sites 607/609 [*Raymo et al.*, 1989], ODP Site 659 [*Tiedemann et al.*, 1994], ODP Site 846/849 [*Shackleton et al.*, 1995; *Schneider*, 1995], ODP Site 983/984 [*Channell and Kleiven*, 2000; *Channell et al.*, 2002] and Italian land sections [*Lourens et al.*, 1996]. The correlations are not always straightforward due to uncertainties in interpretation of either the isotope stratigraphy or the magnetic stratigraphy. At Site 980, the Matuyama-Brunhes lies in MIS 19 and the boundaries of the Jaramillo Chronozone in MIS 27 and MIS 31, consistent with the papers cited above.

[16] Within the Brunhes Chronozone at Site 980, virtual geomagnetic poles (VGPs) cross the equator at ~190 ka and ~690 ka. The younger of the two "events" can be equated to the Iceland Basin Event recorded at ODP Sites 983/984 [*Channell*, 1999], elsewhere in the North Atlantic [*Weeks et al.*, 1995; *Lehman et al.*, 1996; *Nowaczyk and Antonow*, 1997], in the South Atlantic [*Stoner et al.*, 2003] and in the Pacific Ocean [*Yamazaki and Ioka*, 1994; *Roberts et al.*, 1997]. At Site 980, the Iceland Basin Event correlates to the MIS 6/7 boundary as at Sites 983/984 (Table 1). The apparent excursion at Site 980 at ~690 ka is manifest as a change in declination (Figure 3), rather than inclination, within a single core section (980A-8H-3). The ~690 ka "event" will need to be ratified by data from other sites. It may correspond in age to "Event 17α" recognized by *Lund et al.* [2001] in sediments from ODP Leg 172 (western central Atlantic). The durations of the Brunhes-age "events" at Site 980 are ~3 kyr and ~9 kyr, based on the age model (Table 1).

[17] DSDP Site 609 in the central North Atlantic provided the first unequivocal documentation of the Cobb Mountain Subchron in deep-sea sediments [*Clement and Kent*, 1987; *Clement and Martinson*, 1992]. At Site 609, it can be correlated to MIS 35/36 [*Ruddiman et al.*, 1989] (Table 1). This subchron has also been recognized in the North Atlantic [*Clement and Martinson*, 1992; *Yang et al.*, 2001; *Channell et al.*, 2002], in the Celebes and Sulu Seas [*Hsu et al.*, 1990], in the Lau Basin [*Abrahamsen and Sager*, 1994; *Clement*, 2000] and on the California Margin [*Guyodo*

Table 1. Correlation of Subchron Boundaries and Excursions to MIS and Absolute Age[a]

Name of subchron/event	MIS[b] Sites 607, 609, 677	MIS[c] Italy	MIS[d] Sites 983/984	MIS Site 980 (this paper)	Age (ka) Site 980 (this paper)
Iceland Basin Event			6/7 bound.	6/7 bound	190–193
Event 17α				mid 17	687–696
Matuyama-Brunhes bound.	19	19		19	777
Top Jaramillo	mid 27	27	mid 27	mid 27	987
Base Jaramillo	mid 31	31	mid 31	top 31	1060
Top Cobb. Mt.	base 35		mid 35	mid 35	1163
Base Cobb Mt.	base 35		mid 36	base 35	1176

[a] MIS, marine isotope stage.
[b] *Ruddiman et al.* [1989], *Raymo et al.* [1989], *Shackleton et al.* [1990].
[c] *Lourens et al.* [1996].
[d] *Channell* [1999], *Channell and Kleiven* [2000], *Channell et al.* [2002].

et al., 1999]. At Site 980, the Cobb Mountain Subchron can be correlated to MIS 35 and has an estimated duration of 13 kyr (Figure 3, Table 1).

[18] At Hole 980B, the Matuyama-Brunhes boundary and the top Jaramillo polarity transition appear to be well preserved within single cores, 980B-9H and 980B-10H, respectively. For both these polarity transitions, the mean sedimentation rate across the transition is 4 cm/kyr (Figure 2b). The spike in sedimentation rates within MIS 19 (Figure 2b) appears to occur just below the Matuyama-Brunhes boundary. The VGPs pass through the Americas (Figure 10), consistent with the tendency for VGP transition paths to be longitudinally constrained [*Clement*, 1991; *Laj et al.*, 1991]. Both VGP paths from Site 980 show a hang-up (cluster or loop) of VGPs in the South Atlantic region that has also been observed in more detailed transition records from ODP Sites 983/984 [*Channell and Lehman*, 1997]. The more complex VGP paths at Sites 983/984, relative to those from Site 980, can be explained by higher sedimentation rates (~15 cm/kyr) across these polarity transitions at Sites 983/984 [*Channell and Kleiven*, 2000].

[19] Site 980 from the Feni Drift has carbonate percentages that vary widely in the 20–90% range with higher values during interglacial stages (Figure 6), reflecting enhanced surface water productivity. Sites 983/984 from the Gardar and Bjorn Drifts (~700 km NW of Site 980, Figure 1) have lower carbonate percentages in the 10–40% range [*Ortiz et al.*, 1999]. At Site 983/984, the age models indicate that sedimentation rates are sometimes elevated during terminations but not appreciably during interglacial stages [*Channell*, 1999; *Channell and Kleiven*, 2000]. The large fluctuations in carbonate percentage at Site 980 lead to large fluctuations in magnetic concentration parameters (Figure 6) that are not ideal for paleointensity determinations, for reasons mentioned above. The consistency of the Site 980 paleointensity record with those from Sites 983/984 (Figure 8) indicates, however, that a common normalized remanence record can be resolved from the two contrasting sedimentary environments. Discrepancies between the two Site 980 paleointensity proxies (boxed in Figure 8b) are apparent particularly in peak interglacial and glacial stages (MIS 1–2, MIS 6, MIS 11–12 and MIS 18–19) where magnetic concentration and grain size have extreme values.

[20] The Pacific records and Sint-800 stack shown in Figure 8d display some paleointensity features seen in the records from Sites 980/983/984 (Figures 8b and 8c). Numerical simulations have demonstrated that low mean sedimentation rates and/or moderate/poor quality age control can explain not only chronological offsets of paleointensity features, but also differences in amplitude of apparently synchronous features [*Guyodo and Channell*, 2002]. The Pacific records and the Sint-800 stack are relatively smoothed, due to the low mean sedimentation rates associated with them. The Sint-800 stack is a global stack of 19 records with variable quality age control. Most of the Sint-800 records have mean sedimentation rates of a few cm/kyr or less [*Guyodo and Valet*, 1999]. The California margin record (ODP Site 1021) has a

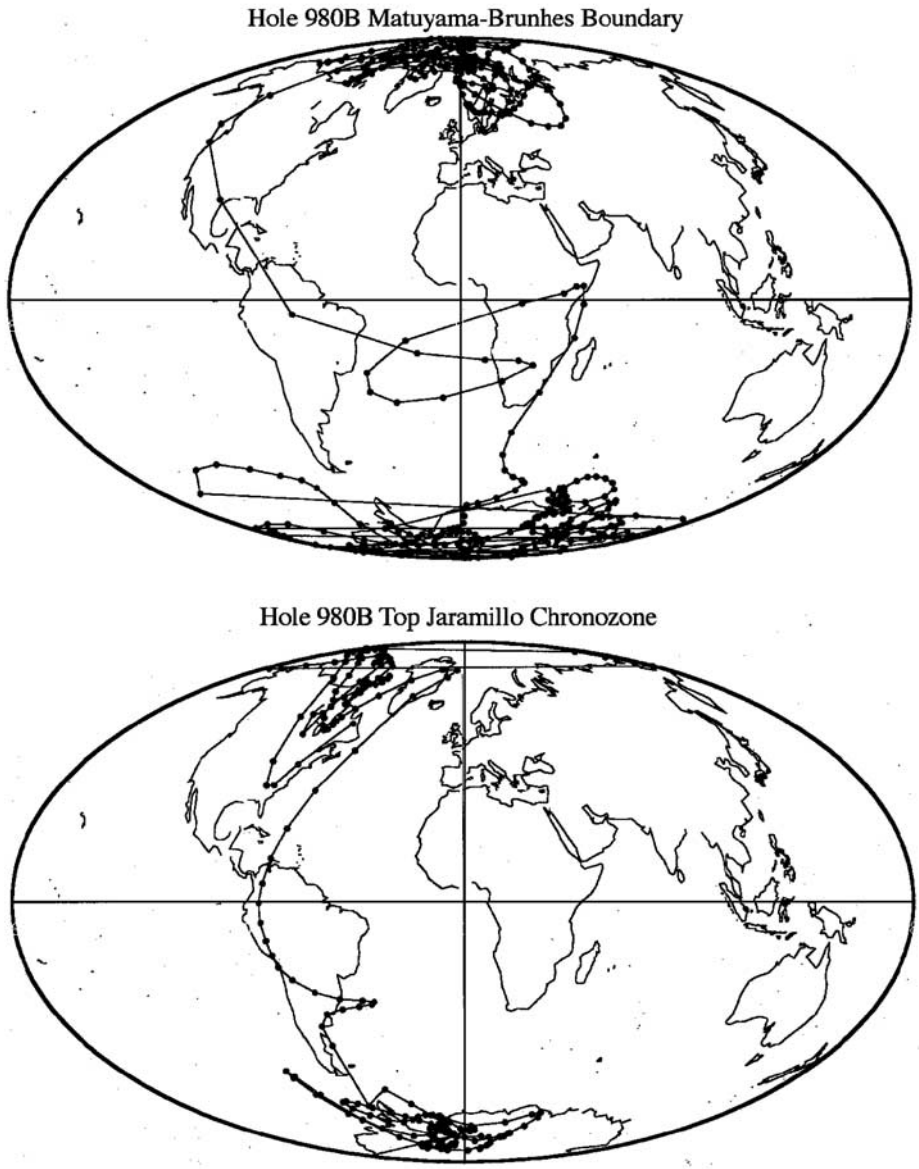

Figure 10. Virtual geomagnetic polar latitudes (VGPs) across the Matuyama-Brunhes boundary and across the reversal at the top of the Jaramillo Chronozone, at Hole 980B. Hammer-Aitoff projection.

Brunhes age model based on a correlation of the susceptibility record to a reference $\delta^{18}O$ curve, and interpolation between reversal boundaries for the Matuyama Chron [*Guyodo et al.*, 1999]. The Site 1021 age model yields a mean sedimentation rate of 3.4 cm/kyr. The age control for the ODP Leg 138 record [*Valet and Meynadier*, 1993; *Meynadier et al.*, 1995] is based on orbital tuning of the GRAPE density stratigraphy [*Shackleton et al.*, 1995]. Mean sedimentation rates over the last 1.2 Myrs for the relevant sites (Sites 848 and 851) are less than 2 cm/kyr. In the case of the Ontong-Java records (ODP Sites 803 and 807), the age models are based on interpolation between reversal boundaries, and mean sedimentation rates are again less than 2 cm/kyr [*Kok and Tauxe*, 1999]. In contrast, mean sedimentation rates for Sites 980, 983 and 984 over the last 1.2 Myrs are 10, 13 and 13 cm/kyr, respectively. We conclude that the records displayed in Figure 8 represent different renditions of

a global geomagnetic paleointensity signal, biased by variable sedimentation rates and variable age control of individual records, and inadequate normalization for some parts of the records.

Acknowledgments

[21] We thank Gary Acton and Joe Stoner for reviews of the manuscript. We are indebted to the staff of the Ocean Drilling Program (ODP) for facilitating this study, and we particularly appreciate the assistance of the staff at the ODP Bremen Core Repository. Research supported by US National Science Foundation (EAR-98-04711).

References

Abrahamsen, N., and W. Sager, Cobb Mountain geomagnetic polarity event and transitions in three deep-sea sediment cores from the Lau Basin, *Proc. Ocean Drill. Program Sci. Results*, *135*, 737–762, 1994.

Channell, J. E. T., Geomagnetic paleointensity and directional secular variation at Ocean Drilling Program (ODP) Site 984 (Bjorn Drift) since 500 ka: Comparisons with ODP Site 983 (Gardar Drift), *J. Geophys. Res.*, *104*, 22,937–22,951, 1999.

Channell, J. E. T., and H. F. Kleiven, Geomagnetic palaeointensities and astrochronological ages for the Matuyama-Brunhes boundary and the boundaries of the Jaramillo Subchron: Palaeomagnetic and oxygen isotope records from ODP Site 983, *Philos. Trans. R. Soc. London Ser. A*, *358*, 1027–1047, 2000.

Channell, J. E. T., and B. Lehman, The last two geomagnetic polarity reversals recorded in high-deposition-rate sediment drifts, *Nature*, *389*, 712–715, 1997.

Channell, J. E. T., and B. Lehman, Magnetic stratigraphy of Leg 162 North Atlantic Sites 980–984, *Proc. Ocean Drill. Program Sci. Results*, *162*, 113–130, 1999.

Channell, J. E. T., D. A. Hodell, J. McManus, and B. Lehman, Orbital modulation of geomagnetic paleointensity, *Nature*, *394*, 464–468, 1998.

Channell, J. E. T., A. Mazaud, P. Sullivan, S. Turner, and M. E. Raymo, Geomagnetic excursions and paleointensities in the Matuyama Chron at Ocean Drilling Program Sites 983 and 984 (Iceland Basin), *J. Geophys. Res.*, *107*(B6), 2114, doi:10.1029/2001JB000491, 2002.

Clement, B. M., Geographical distribution of transitional VGPs: Evidence for non-zonal equatorial symmetry during the Matuyama-Brunhes geomagnetic reversal, *Earth Planet. Sci. Lett.*, *104*, 48–58, 1991.

Clement, B. M., Comment on the Lau Basin Cobb Mountain records by Abrahamsen and Sager, *Phys. Earth Planet. Inter.*, *119*, 173–184, 2000.

Clement, B. M., and D. V. Kent, Short polarity intervals within the Matuyama: Transition field records from hydraulic piston cored sediments from the North Atlantic, *Earth Planet. Sci. Lett.*, *81*, 253–264, 1987.

Clement, B. M., and D. G. Martinson, A quantitative comparison of two paleomagnetic records of the Cobb Mountain subchron from North Atlantic deep-sea sediments, *J. Geophys. Res.*, *97*, 1735–1752, 1992.

Day, R., M. Fuller, and V. A. Schmidt, Hysteresis properties of titanomagnetites: grain-size and compositional dependence, *Phys. Earth Planet. Inter.*, *13*, 260–267, 1977.

Flower, B. P., D. W. Oppo, J. F. McManus, K. A. Venz, D. A. Hodell, and J. A. Cullen, North Atlantic intermediate to deep water circulation and chemical stratification during the past 1 Myr, *Paleoceanography*, *15*, 388–403, 2000.

Guyodo, Y., and J. E. T. Channell, Effects of variable sedimentation rates and age errors on the resolution of sedimentary paleointensity records, *Geochem. Geophys. Geosyst.*, *3*(8), 1048, doi:10.1029/2001GC000211, 2002.

Guyodo, Y., and J.-P. Valet, Global changes in intensity of the earth's magnetic field during the past 800 kyr, *Nature*, *399*, 249–252, 1999.

Guyodo, Y., C. Richter, and J.-P. Valet, Paleointensity record from Pleistocene sediments (1.4–0 Ma) off the California Margin, *J. Geophys. Res.*, *104*, 22,953–22,964, 1999.

Hagelberg, T., N. J. Shackleton, N. Pisias, and Shipboard Scientific Party, Development of composite depth sections for Sites 844 through 854, *Proc. Ocean Drill. Program Inital Rep.*, *138*, 79–85, 1992.

Howard, W. R., A warm future in the past, *Nature*, *388*, 418–419, 1997.

Hsu, V., D. L. Merrill, and H. Shibuya, Paleomagnetic transition records of the Cobb Mountain event from sediment of the Celebes and Sulu seas, *Geophys. Res. Lett.*, *17*, 2069–2072, 1990.

King, J. W., S. K. Banerjee, and J. Marvin, A new rock-magnetic approach to selecting sediments for geomagnetic paleointensity studies: Application to paleointensity for the last 4000 years, *J. Geophys. Res.*, *88*, 5911–5921, 1983.

Kirschvink, J. L., The least squares lines and plane analysis of paleomagnetic data, *Geophys. J. R. Astron. Soc.*, *62*, 699–718, 1980.

Kok, Y. S., and L. Tauxe, A relative geomagnetic paleointensity stack from Ontong-Java Plateau sediments for the Matuyama, *J. Geophys. Res.*, *104*, 25,401–25,413, 1999.

Laj, C., A. Mazaud, R. Weeks, M. Fuller, and E. Herrero-Bervera, Geomagnetic reversal paths, *Nature*, *351*, 447, 1991.

Laskar, J., F. Joutel, and F. Boudin, Orbital, precessional, and insolation quantitites for the Earth from −20 myr to +10 myr, *Astron. Astrophys.*, *270*, 522–533, 1993.

Lehman, B., C. Laj, C. Kissel, A. Mazaud, M. Paterne, and L. Labeyrie, Relative changes of the geomagnetic field intensity during the last 280 k year from piston cores in the Azores area, *Phys. Earth Planet. Int.*, *93*, 269–284, 1996.

Lourens, L. J., A. Antonarakou, F. J. Hilgen, A. A. M. Van Hoof, C. Vergnaud-Grazzini, and W. J. Zachariasse, Evaluation of the Plio-Pleistocene astronomical timescale, *Paleoceanography*, *11*, 391–413, 1996.

Lund, S. P., T. Williams, G. D. Acton, B. Clement, and M. Okada, Brunhes chron magnetic field excursions from Leg 172 sediments, *Proc. Ocean Drill. Program Sci. Results*, *172*, 1–18, 2001.

Manley, P. L., and D. W. Caress, Mudwaves on the Gardar Sediment Drift, NE Atlantic, *Paleoceanography*, *9*, 973–988, 1994.

McCave, I. N., P. F. Lonsdale, C. D. Hollister, and W. D. Gardner, Sediment transport over the Hatton and Gardar contourite drifts, *J. Sediment. Petrol.*, *50*, 1049–1062, 1980.

McManus, J., D. W. Oppo, and J. L. Cullen, A 0.5-Million-Year record of Millennial-Scale climate variability in the North Atlantic, *Science*, *283*, 971–974, 1999.

Meynadier, L., J.-P. Valet, and N. J. Shackleton, Relative geomagnetic intensity during the last 4 M.Y. from the equatorial Pacific, *Proc. Ocean Drill. Program Sci. Results*, *138*, 779–793, 1995.

Nowaczyk, N. R., and M. Antonow, High resolution magnetostratigraphy of four sediment cores from the Greenland Sea, I, Identification of the Mono Lake excursion, Laschamp and Biwa I/Jamaica geomagnetic polarity events, *Geophys. J. Int.*, *131*, 310–324, 1997.

Oppo, D. W., J. F. McManus, and J. L. Cullen, Abrupt climate events 500,000–340,000 years ago: Evidence from subpolar North Atlantic sediments, *Science*, *279*, 1335–1338, 1998.

Ortiz, J., A. Mix, S. Harris, and S. O'Connell, Diffuse spectral reflectance as a proxy for percent carbonate content in north Atlantic sediments, *Paleoceanography*, *14*, 171–186, 1999.

Paillard, D., L. Labeyrie, and P. Yiou, Macintosh program performs time-series analysis, *Eos Trans. AGU*, *77*, 379, 1996.

Raymo, M. E., W. F. Ruddiman, J. Backman, B. M. Clement, and D. G. Martinson, Late Pliocene variation in Northern Hemisphere ice sheets and North Atlantic deep water circulation, *Paleoceanography*, *4*, 413–446, 1989.

Roberts, A. P., B. Lehman, R. J. Weeks, K. L. Verosub, and C. Laj, Relative paleointensity of the geomagnetic field over the last 200,000 years from ODP Sites 883 and 884, North Pacific Ocean, *Earth Planet. Sci. Lett.*, *152*, 11–23, 1997.

Ruddiman, W. F., M. E. Raymo, D. G. Martinson, B. M. Clement, and J. Backman, Pleistocene evolution: Northern hemisphere ice sheet and north Atlantic ocean, *Paleoceanography*, *4*, 353–412, 1989.

Schneider, D. A., Paleomagnetism of some Leg 138 sediments: Detailing Miocene magnetostratigraphy, *Proc. Ocean Drill. Program Sci. Results*, *138*, 59–72, 1995.

Shackleton, N. J., and N. G. Pisias, Atmospheric carbon dioxide, orbital forcing, and climate, in *The Carbon Cycle and Atmospheric CO_2: Natural Variations Archean to Present*, *Geophys. Monogr. Ser.*, vol. 32, edited by E. T. Sundquist and W. S. Broeker, pp. 412–417, AGU, Washington, D.C., 1985.

Shackleton, N. J., A. Berger, and W. R. Peltier, An alternative astronomical calibration of the lower Pleistocene timescale based on ODP Site 677, *Trans. R. Soc. Edinburgh Earth Sci.*, *81*, 251–261, 1990.

Shackleton, N. J., S. Crowhurst, T. Hagelberg, N. G. Pisias, and D. A. Schneider, A new Late Neogene time scale: Application to Leg 138 sites, *Proc. Ocean Drill. Program Sci. Results*, *138*, 73–101, 1995.

Shipboard Scientific Party, Site 980/981, *Proc. Ocean Drill. Program Inital Rep.*, *162*, 49–90, 1996.

Stoner, J. S., J. E. T. Channell, D. A. Hodell, and C. D. Charles, A 580 kyr paleomagnetic record from the sub-Antarctic South Atlantic (ODP Site 1089), *J. Geophys. Res.*, in press, 2003.

Tauxe, L., Sedimentary records of relative paleointensity of the geomagnetic field: Theory and practice, *Rev. Geophys.*, *31*, 319–354, 1993.

Tiedemann, R., M. Sarnthein, and N. J. Shackleton, Astronomic timescale for the Pliocene Atlantic $\delta^{18}O$ and dust flux records of Ocean Drilling Program Site 659, *Paleoceanography*, *9*, 619–638, 1994.

Valet, J. P., and L. Meynadier, Geomagnetic field intensity and reversals during the past four million years, *Nature*, *366*, 234–238, 1993.

Weeks, R., C. Laj, L. Endignoux, M. Fuller, A. Roberts, R. Manganne, E. Blanchard, and W. Goree, Improvements in long-core measurement techniques: Applications in palaeomagnetism and palaeoceanography, *Geophys. J. Int.*, *114*, 651–662, 1993.

Weeks, R., C. Laj, L. Endignoux, A. Mazaud, L. Labeyrie, A. Roberts, C. Kissel, and E. Blanchard, Normalized NRM intensity during the last 240,000 years in piston cores from central North Atlantic Ocean: Geomagnetic field intensity or environmental signal?, *Phys. Earth Planet. Inter.*, *87*, 213–229, 1995.

Yamazaki, T., and N. Ioka, Long-term secular variation of the geomagnetic field during the last 200 kyr recorded in sediment cores from the western equatorial Pacific, *Earth Planet. Sci. Lett.*, *128*, 527–544, 1994.

Yang, Z., B. M. Clement, G. D. Acton, S. P. Lund, M. Okada, and T. Williams, Records of the Cobb Mountain Subchron from the Bermuda Rise (ODP Leg 172), *Earth Planet. Sci. Lett.*, *193*, 303–313, 2001.